Three "G's" for Soil–Bedrock Depth Interpretations

Jim Doolittle, Debbie Surabian, Shawn McVey, and Donald Parizek

A relatively new development in ground-penetrating radar (GPR) technology could significantly change the way soil scientists collect, interpret, and store some soil data. A new mapping module included in GPR processing software allows the georeferencing of GPR data collected with a suitable global positioning system (GPS) receiver. We discuss these improvements in GPR technology as well as initial field experiments, which involved interpretation of the depth to bedrock in areas of Nipmuck, Brimfield, and Brookfield soils in northeastern Connecticut. These experiments represent the first known merger of GPR, GPS, and geographic information system (GIS) technologies—the three "G's"—within USDA. The synergistic use of these technologies permits the collection of large, tabular, georeferenced GPR data sets, which can be stored, manipulated, analyzed, and displayed in GIS. These collection, analysis, and display formats should greatly improve the utility of GPR within the Soil Survey Program. Many MLRA offices will find the integrated use of these evolving technologies a great leap forward in addressing depth to bedrock issues, map unit composition (based on soil depth criterion), and other quality control concerns.

Background

One of the most effective uses of GPR within the soil survey program has been the estimation of bedrock depths. In many upland areas, it is difficult to excavate and examine soil profiles and determine the depth to bedrock. Rock fragments slow and limit the effectiveness of conventional soil surveying tools (tiling spades, augers, and probes). Frequently, in many upland areas, soil scientists are uncertain as to whether auger refusal was caused by bedrock or a large rock fragment. Limited by conventional soil survey tools, soil scientists infer the depth to bedrock from vegetative cover, nearby exposures, and/or landscape position. These inferences are often based on associated or anticipated, rather than confirmed depths to bedrock. Studies have shown that the depth to bedrock is underestimated with traditional soil survey tools (Schellentrager and Doolittle, 1991; Collins et al., 1989; Doolittle et al., 1988).

Conventional soil survey tools provide only limited or partial information. Observations are limited in depth and number, and are widely spaced. Soil scientist must make interpretations based on inferences made across the extensive areas between cores. Even within intensely surveyed areas, the spacing between cores is often too large to adequately characterize the spatial variability of the underlying soil–bedrock interface.

For many years, GPR has been used effectively in upland areas to extend the depth of observation and improve the quality of soil–bedrock information. GPR provides high-resolution information that can assist interpretations and the extrapolation of information obtained with traditional surveying techniques (Davis and Annan, 1989). GPR has been used to chart bedrock depths (Schellentrager and Doolittle, 1991; Collins et al., 1989; Davis and Annan, 1989; Doolittle et al., 1988). In addition, GPR has been used to detect geologic hazards in advance of mining operations (Grodner, 2001; Molinda et al., 1996), locate and characterize fracture patterns in crystalline bedrock (Lane et al., 2000; Stevens et al., 1995; Holloway and Mugford, 1990), and identify cavities, sinkholes, and fractures in limestone (Pipan et al., 2000; Doolittle and Collins, 1998; Barr, 1993). Recently, GPR has been used to study weathered bedrock and the transition from weathered to hard bedrock (Aranha et al., 2002; Li, 1998).

Olson and Doolittle (1985) observed that GPR can provide continuous, highly interpretable images of the bedrock surface to depths of 3 m in medium-textured, upland soils. Collins et al. (1989) demonstrated that GPR was more reliable and effective than soil augers used by a soil scientist to map bedrock depths. In their study, the average difference between actual and radar-interpreted depths to bedrock was only 6 cm, with 87% of the observations within 10 cm. Where depths to bedrock are less than 4 m, Birkhead et al. (1996) observed an average error between observed and radar interpreted measurements of 4.4%.

MLRA offices will find the integrated use of these evolving technologies a great leap forward in addressing depth to bedrock issues, map unit composition... and other quality control concerns.

J. Doolittle, Research Soil Scientist, USDA-NRCS-NSSC, Newtown Square, PA (Jim.Doolittle@lin.usda.gov); D. Surabian, Soil Scientist, USDA-NRCS, Tolland, CT; S. McVey, Assistant State Soil Scientist, USDA-NRCS, Tolland, CT; and D Parizek, Soil Scientist, USDA-NRCS, Windsor, CT.
Published in Soil Surv. Horiz. 50:25–29 (2009).

Study Sites

Two study sites were selected in northeastern Tolland County, Connecticut. Site 1 is located in the town of Willington. Here, the majority of the area traversed with GPR was mapped as Hollis–Chatfield–Rock outcrop complex, 15 to 45% slopes (75E), but small areas of Hollis–Chatfield–Rock outcrop complex, 3 to 15% slopes (73C), and Fluvaquents–Udifluvents Complex, frequently flooded (109) were included in the radar traverse. In this area, Map Unit 75E is being recorrelated as Map Unit 71E, Nipmuck–Brimfield–Rock outcrop, 15 to 45% slopes, and Map Unit 73C is being recorrelated as Map Unit 72C, Nipmuck–Brookfield complex, 3 to 15% slopes, very bouldery.

Site 2 is located in the town of Union. Here, the majority of the area traverses with GPR was mapped as Brookfield–Brimfield–Rock outcrop complex, 15 to 45% slopes (71E), but areas of Sutton fine sandy loam, 2 to 15% slopes, extremely stony (52C) and Charlton–Chatfield complex, 15 to 45% slopes, very rocky (73E) were included in the radar traverse. Map Unit 71E is also being recorrelated as Nipmuck–Brimfield–Rock outcrop, 15 to 45% slopes, and Map Unit 73E is being recorrelated as Map Unit 72E, Nipmuck–Brookfield complex, 15 to 45% slopes, very bouldery.

The very deep, well-drained Brookfield, moderately deep, well-drained Nipmuck, and the shallow, somewhat excessively drained Brimfield soils formed in till derived mainly from iron-sulfide bearing schist (Soil Survey Staff, 2008). Brookfield, Brimfield, and Nipmuck soils have parasesquic mineralogy and are thought to be postactive sulfate soils, the final stage of the acid sulfate weathering process. The acid sulfate weathering process explains the high pedogenic iron content and resulting parasesquic mineralogy. The very deep, moderately well-drained Sutton soils formed in till (Soil Survey Staff, 2008). The taxonomic classifications of the aforementioned soil series are listed in Table 1. Fluvaquents and Udifluvents formed in alluvial sediments subject to flooding and are found occupying small, narrow stream valleys on glaciated uplands.

Equipment

The radar unit is the TerraSIRch Subsurface Interface Radar (SIR) System-3000 (SIR-3000) manufactured by Geophysical Survey Systems, Inc. (GSSI, Salem, NH).[1] The SIR-3000 consists of a digital control unit (DC-3000) with keypad, SVGA video screen, and connector panel. A 10.8-V lithium-ion rechargeable battery powers the system. The SIR-3000 weighs about 9 lb. (4.1 kg) and is backpack portable. With an antenna, the SIR-3000 requires two people to operate. Daniels (2004) discussed the use and operation of GPR. An antenna with a center frequency of 200 MHz was used in this study.

A Trimble AG114 GPS receiver was used to collect position data along each GPR traverse line. Using the RADAN (version 6.6) software (GSSI), these coordinates were attached to GPR profile data.[1]

Table 1. Soil taxonomic classification.

Soil series	Taxonomic classification
Brimfield	Loamy, parasesquic, mesic Lithic Dystrudepts
Brookfield	Coarse-loamy, parasesquic, mesic Typic Dystrudepts
Chatfield	Coarse-loamy, mixed, superactive, mesic Typic Dystrudepts
Hollis	Loamy, mixed, active, mesic Lithic Dystrudepts
Nipmuck	Coarse-loamy, parasesquic, mesic Typic Dystrudepts
Sutton	Coarse-loamy, mixed, active, mesic Aquic Dystrudepts

Survey Procedures

GPR traverse lines were established at each site. Before the integration of GPR and GPS, traverse lines were selected in representative portions of soil polygons. Along a GPR traverse line, equally spaced observation points were measured or paced-off. The spacing of these observation points varied with the anticipated complexity of soil properties or soil patterns and ranged from one to several tens of meters. The number of observations points depended on the length of the GPR traverse line, but typically ranged from 10 to 25 observations. At each observation point, the radar operator impressed a mark on the radar record to indicate a measurement point. Later, during the postsurveying analysis of the radar record, the depth to bedrock would be interpreted at each measurement point and manually entered into a spreadsheet. Basic statistics for each traverse line would be developed by the radar operator and presented to the soil survey project leader.

During the 1990s, it was realized that GPR data needed to be more fully integrated with available soil data and maps. A logical trend was to integrate GPR with GPS. As noted by Rial et al. (2005), under favorable conditions GPR–GPS integration allows for the accurate positioning of radar data and its importation into GIS. However, this integration was waiting on developments to occur in both technologies. These developments have now occurred. A new mapping module included in GPR processing software provides the capability of not only "visually georeferencing GPR data" (GSSI, 2008), but "widening the scope of GPR surveys" (Gustafsson, 2007).

With GPS, observation points no longer need to be measured or paced-off. As the radar is moved across a soil polygon, its position is tracked with GPS. The number and distance between potential observation points is determined by the speed of advance and the sampling frequency set on the radar unit. The sampling frequency or rate is the number of scans that the GPR system will record in a given period of time. A scan or trace is a series of reflected radar waveforms derived from one transmitted pulse. The scan rate is used to adjust the level of resolution; the higher the sampling rate, the greater the number of "hits" on a target, and the more likely (within certain constraints) that smaller-sized features will be detected with GPR. GPR readings (scans) are not continuous, but are taken at set intervals along traverse lines. In this study, because of the highly irregular nature of the bedrock surface and the presence of scattering bodies (e.g., rock fragments, tree roots) within the soils, the scanning rate was set to 60 scans/s. Position data were recorded at a rate of one measurement/s with the AG114 GPS receiver. During postsurveying processing of radar data, the position of each radar scan is proportionally adjusted according to the time stamp of the two nearest positions recorded with the GPS receiver. As each scan of the radar is georeferenced, the integration of GPS with GPR results in an unimaginably large data set (91,981 georeferenced data points were collected in this study).

There are some drawbacks to this process of integrating GPS with GPR data. Although GPS receivers might need only three satellites, the SIR-3000 requires a minimum of four satellites to somewhat accurately triangulate locations and provide a good solution. Any less and the GPS data will not be recorded. In addition, GPS signal reception is critical at the start and end of each radar traverse, as the first and last positions must be stored in the header of each radar file. This is often difficult in

[1] Manufacturers' names are provided for specific information; use does not constitute endorsement.

forested areas or terrains with substantial relief. When working in areas of low satellite visibility, some GPS data will be lost (i.e., bad signal). During postprocessing, GPR data will be interpolated among the known GPS positions. When possible, the use of GPR and GPS in forested terrains should be scheduled for when there are not leaves on the trees.

At the two study sites, GPR traverses were conducted along trails that passed through forested terrains with moderate relief. Along these forested trails, the 200-MHz antenna provided a stable platform and remained closely coupled to the ground surface. This helped to reduce unwanted background noise caused by the jarring and uncoupling of the antenna with the soil surface. Each radar traverse was stored as a separate file. Radar records were reviewed in the field and the soil–bedrock interface identified.

Calibration of GPR

Ground-penetrating radar is a time-scaled system. The system measures the time that it takes electromagnetic energy to travel from an antenna to an interface (e.g., bedrock, soil horizon, stratigraphic layer) and back. To convert the travel time into a depth scale, either the velocity of pulse propagation or the depth to a reflector must be known. The relationships among depth (D), two-way pulse travel time (T), and velocity of propagation (v) are described in Eq. [1] (after Daniels, 2004):

$$v = 2D/T \qquad [1]$$

The velocity of propagation is principally affected by the relative dielectric permittivity (E_r) of the profiled material(s) according to Eq. [2] (after Daniels, 2004):

$$E_r = (C/v)^2 \qquad [2]$$

where C is the velocity of propagation in a vacuum (0.298 m/ns). Velocity is expressed in meters per nanosecond. In soils, the amount and physical state (temperature dependent) of water have the greatest effect on the E_r and v.

Based on the measured depth and the two-way pulse travel time to a known subsurface reflector (buried plate at 40 cm), the velocity of propagation and the relative dielectric permittivity through the upper part of the soil profile were estimated using Eq. [1] and [2]. An estimated E_r of 5.19 resulted in a v of 0.1308 m/ns. Using a constant v of 0.1308 m/ns, a range of 75 ns, and Eq. [1], the 200-MHz antenna was set to penetrate the subsurface to a depth of about 4.9 m

Collected GPR Data

The SIR-3000 system provides a setup for the simultaneous use of a GPS receiver and serial data recorder (SDR). With this setup, each scan on radar records can be georeferenced (position/time matched). Using the Interactive Interpretation module of the RADAN processing software, depths to the soil–bedrock interface were quickly and reasonably accurately picked and automatically outputted to a worksheet (*X, Y, Z* format; containing latitude, longitude, and depths to bedrock, and other useful data). An example of a small portion of the data set that was recorded in this study is shown in Table 2. As evident from the positions (columns 2 and 3) of the sequentially numbered radar scans (column 1) in Table 2, the system hardly moved in the time required to collect the 17 radar scans shown in this example. In Table 2, Amplitude (column 5) represents the strength of the GPR signal wave that was picked. Higher amplitude represents a stronger radar response to the interface, and typically greater and more abruptly contrasting dielectric properties between the materials. In Table 2, the two-way travel time is displayed in column 7. The interpreted depth to the soil–bedrock interface (column 4) was automatically estimated and entered into the spreadsheet using the estimated velocity of propagation (v = 0.1308 m/ns, column 6), the two-way travel time to the picked interface (column 7), and Eq. [1]. Using the Interactive Interpretation module, data can be easily exported into GIS for plotting and visualization.

Results

Figure 1 is a representative radar record from an area of Nipmuck–Brimfield–Rock outcrop, 15 to 45% slopes, which was collected at Site 2. In Fig. 1, the contact of the soil materials with the underlying schist bedrock has been highlighted with a green-colored line. This contact forms a well-expressed, high-amplitude, continuous reflector that is easily followed across this portion of the radar record. In some portions of this radar record, the soil–bedrock interface was more irregular, segmented, variable in signal amplitude, and, as a consequence, not as easily identified. Because of the lack of a single, well-expressed, continuous, high-amplitude reflection, the identification

Table 2. Shown is a portion of the data, which is picked from the radar record and exported using the Interactive Interpretation Module of the RADAN processing software.

Scan	Longitude	Latitude	Depth	Amplitude	v	t
			m		m/ns	ns
16	−72.282872	41.8900564	1.41	14	0.13	21.68
17	−72.2828719	41.8900564	1.41	15	0.13	21.68
18	−72.2828719	41.8900564	1.41	13	0.13	21.68
19	−72.2828718	41.8900564	1.41	18	0.13	21.68
20	−72.2828718	41.8900564	1.41	20	0.13	21.68
21	−72.2828718	41.8900564	1.41	19	0.13	21.68
22	−72.2828717	41.8900564	1.41	18	0.13	21.68
23	−72.2828717	41.8900564	1.41	22	0.13	21.68
24	−72.2828716	41.8900564	1.41	25	0.13	21.68
25	−72.2828716	41.8900564	1.40	22	0.13	21.53
26	−72.2828715	41.8900564	1.40	12	0.13	21.53
27	−72.2828715	41.8900564	1.40	14	0.13	21.53
28	−72.2828715	41.8900564	1.40	13	0.13	21.53
29	−72.2828714	41.8900564	1.40	15	0.13	21.53
30	−72.2828714	41.8900564	1.40	9	0.13	21.53
31	−72.2828713	41.8900564	1.40	10	0.13	21.53
32	−72.2828713	41.8900564	1.40	9	0.13	21.53

Fig. 1. In this radar record from an area of Nipmuck–Brimfield–Rock outcrop, 15 to 45% slopes, the bedrock surface has been highlighted with a green line.

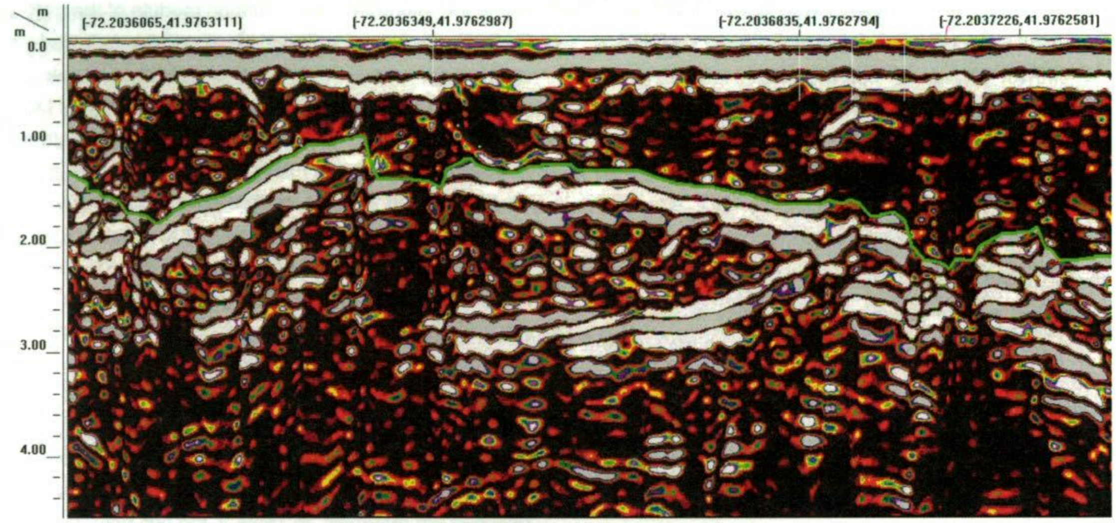

Fig. 2. These images were prepared by importing georeferenced GPR data into ArcGIS 9.2. Each image shows the location of the GPR traverse lines. Different colors are used to show the different depths (by soil depth classes) to bedrock along the traverse lines.

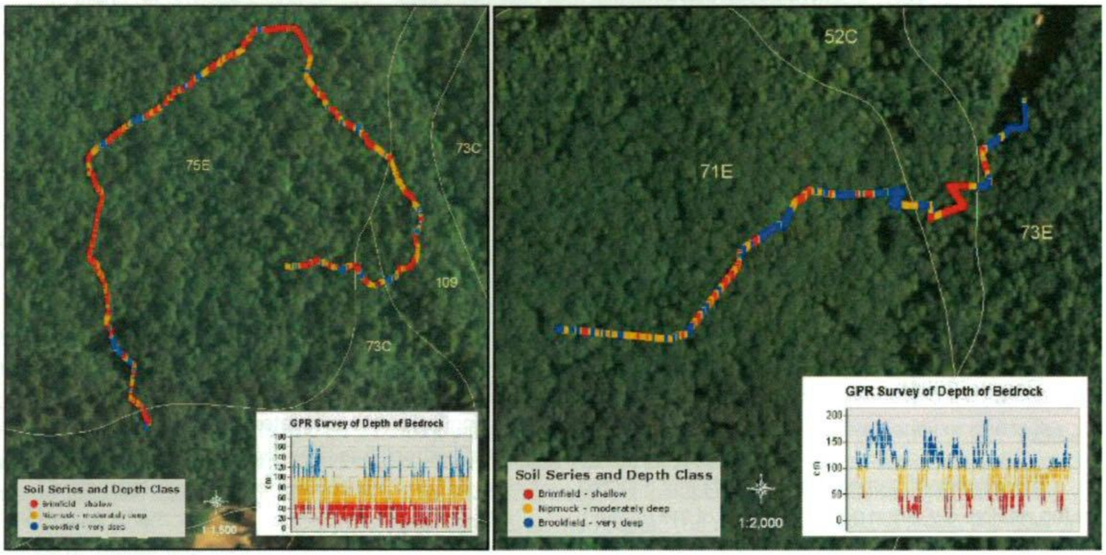

of the soil–bedrock interface is more unclear in these portions of the radar records, and consequently, the accuracy of interpreted soil depth measurements is lessened. However, considering the limitations of traditional soil survey tools (spade and auger), and the interpretive nature and uncertainty associated with coring for bedrock in tills that contain large amounts of rock fragments, radar interpretations, even in areas of ambiguity, are considered no less accurate, but infinitely faster and easier to collect.

Table 3 provides the basic statistics for the radar traverses completed at Sites 1 and 2. For a survey that required only minutes to complete in the field, the number of observation is incredible. For both sites, the average depth to bedrock was moderately deep (50–100 cm). At Site 1, the averaged depth to bedrock was 60 cm, with a range of 0 to 176 cm. One-half of the recorded depth measurements had depths to bedrock between 30 and 88 cm. At Site 2, the averaged depth to bedrock was 98 cm, with a range of 0 to 196 cm. One-half of the recorded depth measurements had depths to bedrock between 70 and 127 cm.

Table 4 provides the frequency distribution of the radar measurements based on soil depth criterion for the two sites. At Site 1, soils are shallow (0–50 cm) at 45% and moderately deep at 39% of the measurement points (Table 4). At Site 1, deep (100–150 cm) and very deep (>150 cm) soils represent minor inclusions and make up about 16% of the measurement points. At Site 2, based on soil depth classes, deep (40%) and moderately deep (31%) soils are codominant. At Site 2, soils are shallow at 17% and very deep at 11% of the measurement points.

Integration of GPR with GIS

The data from the GPR traverses were stored as in an Excel (.xls) file. To ensure that ArcMap 9.2 could read the imported data, columns containing the Longitude (*X*) and Latitude (*Y*) values were formatted as NUMBER, with a minimum of eight decimal places. Before importing into ArcMap 9.2, the output file must also have each column labeled (e.g., ID, Longitude, Latitude, and Depth). The data from the .xls file is added to ArcMap 9.2 using the option: Tools > Add

Table 3. Depth to bedrock statistics for the GPR traverses that were completed at Sites 1 and 2.

	Site 1	Site 2
Number	65526	26455
Average	0.60	0.98
Standard Deviation	0.37	0.42
Minimum	0.00	0.00
25%-tile	0.30	0.70
75%-tile	0.88	1.27
Maximum	1.76	1.96

Table 4. Frequency distribution of observations

	Site 1	Site 2
Shallow	45%	17%
Moderately Deep	39%	31%
Deep	15%	40%
Very Deep	1%	11%

XY Data and then setting the column labeled Longitude as *X* and Latitude as *Y*. Once added, the Spatial Reference Properties dialog box can be opened and a coordinate system for the data selected. Most frequently GPS data are collected on the WGS 1984 datum. After defining the projection, the *XY* Data are added and the points drawn as an event theme in ArcMap. The points can then be exported to a geodatabase feature class, or to a shape file. During this process, the data can also be reprojected to the coordinate system of the ArcMap Data Frame

The images shown in Fig. 2 were prepared following the aforementioned procedures. This represents the first known projection of relevant soil data through the merger of GPR, GPS, and GIS technologies within USDA. It is anticipated that the large, tabular, georeferenced GPR data sets and availability of meaningful display formats within ArcMap GIS should greatly improve the utility of GPR within the Soil Survey Program. Many MLRA offices should find the integrated use of these evolving "3-G" technologies a great leap forward in addressing depth to bedrock issues, map unit composition, and other quality control concerns.

References

Aranha, P.R.A., C.H.R.R. Augustin, and F.G. Sobreira. 2002. The use of GPR for characterizing underground weathered profiles in the sub-humid tropics. J. Appl. Geophys. 49:195–210.

Barr, G.L. 1993. Application of ground-penetrating radar methods in determining hydrogeologic conditions in a karst area, west-central Florida. USGS Water Resources Rep. 92-4141. Tallahassee, FL.

Birkhead, A.L., G.L. Heritage, H. White, and A.W. van Niekerk. 1996. Ground-penetrating radar as a tool for mapping the phreatic surface, bedrock profile, and alluvial stratigraphy in the Sabie River. Kruger National Park. J. Soil Water Conserv. 51(3):234–241.

Collins, M.E., J.A. Doolittle, and R.V. Rourke. 1989. Mapping depth to bedrock on a glaciated landscape with ground-penetrating radar. Soil Sci. Soc. Am. J. 53:1806–1812.

Daniels, D.J. 2004. Ground penetrating radar. 2nd ed. Inst. Electrical Engineers, London, UK.

Davis, J.L., and A.P. Annan. 1989. Ground-penetrating radar for high-resolution mapping of soil and rock stratigraphy. Geophys. Prospect. 37:531–551.

Doolittle, J.A., and M.E. Collins. 1998. A comparison of EM induction and GPR methods in areas of karst. Geoderma 85:83–102.

Doolittle, J.A., R.A. Rebertus, G.B. Jordan, E.I. Swenson, and W.H. Taylor. 1988. Improving soil-landscape models by systematic sampling with ground-penetrating radar. Soil Surv. Horiz. 29:46–54.

Grodner, M. 2001. Using ground penetrating radar to quantify changes in fracture pattern associated with a simulated rockburst experiment. J. S. Afr. Inst. Min. Metallurg. 101(5):261–266.

GSSI. 2008. New mapping module for RADAN 6. Subsurface solutions, Official newsletter of Geophysical Survey Systems, Inc., May 2008, p. 4.

Gustafsson, J. 2007. Widening the scope of GPR surveys. Geo-Drill. Int. 136:26–27.

Holloway, A.L., and J.C. Mugford. 1990. Fracture characterization in granite using ground probing radar. CIM Bull. 83(940):61–70.

Lane, J.W., Jr., M.L. Buursink, F.P. Haeni, and R.J. Versteeg. 2000. Evaluation of ground-penetrating radar to detect free-phase hydrocarbons in fractured rocks– results of numerical modeling and physical experiments. Ground Water 38(6):929–938.

Li, Z. 1998. Applications of ground penetrating radar in Three Gorges Project. p. 209–213. *In* R.G. Plumb (ed.) Proceedings Seventh International Conference on Ground-Penetrating Radar, Lawrence, KS. 27–30 May 1998. Radar Systems and Remote Sensing Lab., University of Kansas.

Molinda, G.M., W.D. Monaghan, G.L. Mowrey, and G.F. Persetic. 1996. Using ground penetrating radar for roof hazard detection in underground mines. RI 9625. USDOE, Pittsburgh Research Center, PA.

Olson, C.G., and J.A. Doolittle. 1985. Geophysical techniques for reconnaissance investigations of soils and surficial deposits in mountainous terrain. Soil Sci. Soc. Am. J. 49:1490–1498.

Pipan, M., L. Baradello, E. Forte, and A. Prizzon. 2000. GPR study of bedding planes, fractures and cavities in limestone. p. 682–687. *In* D. Noon (ed.) Proceedings Eight International Conference on Ground-Penetrating Radar. Goldcoast, Queensland, Australia. 23–26 May 2000. The University of Queensland, Brisbane, QLD, Australia.

Rial, F.I., M. Pereira, H. Lorenzo, and P. Arias. 2005. Acquisition and synchronism of GPR and GPS data. Application on road evaluation. *In* L. Bruzzone (ed.) Image and Signal Processing for Remote Sensing XI, Bruges, Belgium. 20–22 Sept. 2006. Proc. SPIE Vol. 5982.

Schellentrager, G.W., and J.A. Doolittle. 1991. Systematic sampling using ground-penetrating radar to study regional variation of a soil map unit. p. 199–214. *In* M.J. Mausbach and L.P. Wilding (ed.) Spatial variabilities of soils and landforms. SSSA Spec. Publ. 28. SSSA, Madison, WI.

Soil Survey Staff. 2008. Official Soil Series Descriptions. Available sy http://soils.usda.gov/technical/classification/osd/index.html (accessed 10 June 2008, verified 2 Mar. 2009). USDA-NRCS, Lincoln, NE.

Stevens, K.M., G.S. Lodha, A.L. Holloway, and N.M. Soonawala. 1995. The application of ground penetrating radar for mapping fractures in plutonic rocks within the Whiteshell Research Area, Pinawa, Manitoba, Canada. J. Appl. Geophys. 33:125–141.